

PHYSICAL REVIEW LETTERS

VOLUME 17

7 NOVEMBER 1966

NUMBER 19

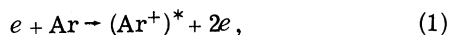
DIRECT ELECTRON EXCITATION CROSS SECTIONS PERTINENT TO THE ARGON ION LASER*†

W. R. Bennett, Jr.,‡ G. N. Mercer, P. J. Kindlmann, B. Wexler, and H. Hyman
Sloane and Dunham Laboratories, Yale University, New Haven, Connecticut

(Received 26 September 1966)

Absolute direct excitation cross sections from the neutral ground state have been measured for upper levels of the strongest laser transitions in Ar II to within errors of $\approx 20\%$. Reasonable agreement is obtained with calculated values of these cross sections based on the "sudden" approximation made by Koozekanani with Hartree-Fock wave functions and intermediate coupling.

It has been previously noted^{1,2} that application of the "sudden perturbation" approximation to collisions between fast electrons and neutrals, of the type



predicts preferential excitation of the $3p^44p$ configuration over the $3p^44s$ with cross sections for individual levels of the order of one percent of the total ionization cross section. We also noted² that the selective nature of the excitation process, when combined with the transition probabilities involved, would lead to population inversions on many transitions of Ar II of the type $4p - 4s$ falling in the blue-green portion of the spectrum. Koozekanani³ has recently performed extensive numerical calculations based on Hartree-Fock wave functions and intermediate coupling in the "sudden" approximation which are in reasonable agreement with our earlier, more qualitative estimate of these cross sections. It has also since been found that nearly all of the known pulsed ion-laser transitions originate in precisely those configurations which would be expected on the basis of the "sudden" approximation in going from one to the next higher state of ionization.⁴

Aside from the work in helium,^{5,6} there are

essentially no previous experimental data available for absolute excitation cross sections in reactions such as (1) above. It is therefore of basic interest to see how precisely the predictions of the sudden approximation agree with experiment in a complicated atom such as argon. It is clear that this approximation must fail at low enough energies. However, it is not obvious a priori how badly it will fail at energies near the peak of the total ionization cross section or at energies typically involved in argon ion lasers.

Since the argon ion laser is the most intense continuous source of coherent radiation in the visible spectrum and since a multitude of processes must be considered for an accurate understanding of the excitation mechanisms in the extremely high-current discharges used,^{4,7} it is of additional importance to determine the absolute values and energy dependence of the cross sections for reaction (1) leading to the more important upper laser levels. For the purpose of determining the relative yield of single- and two-step excitation processes in these lasers, it is in fact desirable to have cross-section data which include all radiative cascade contributions to the upper laser state arising from single electron collisions. These

data are presented below.

In our experiment a triode electron-gun structure is operated in a diode-connected mode with total emission currents of ≤ 0.4 mA/cm². The electron current flowing externally between the grid and plate is measured and used to determine the incident electron flux. Small corrections are made to account for ionization effects, using the average of the total ionization cross sections as reviewed by Kieffer and Dunn.⁸ These corrections include subtraction of the ion current from the measured current to determine the incident electron flux, and allowance for depletion of the high-energy electron flux in the excitation region due to ionization. Pressures are measured with a capacitance manometer and the gas densities are determined using the average temperature measured by thermocouples attached to the grid and plate electrodes. The gun utilizes an oxide-coated cathode of 20 cm² area and is attached to a bakable vacuum system containing reagent-grade argon samples further purified with barium.

Two basic types of data have been taken:

- (a) relative data near threshold from which the appearance potentials are determined, and
- (b) absolute cross-section data taken about the peak in the total ionization cross section from which comparisons with the sudden approximation are made.

The excitation-function data in Fig. 1 were taken with a multichannel counting system which was triggered by a periodic sawtooth applied between the cathode and grid-plate structure. A correction for the variation of electron current with voltage was made numerically. Data for states such as the $4p^2P_{3/2}^{\circ}$ and $4p^2P_{1/2}^{\circ}$ show a roughly linear dependence on the energy above threshold and a fairly sharp intercept at the known energy for reaction (1). These states would be expected with the highest probability on the basis of the sudden approximation and *LS* coupling. At the opposite extreme, a state such as the $4p^4D_{5/2}^{\circ}$ shows a nearly cubic variation above threshold and a number of sharp breaks in the excitation function, suggesting strong radiative cascade contributions from higher-lying levels. Direct, noncascade excitation of this state would be ruled out by angular orthogonality in any coupling scheme in the sudden approximation.

The data for most transitions exhibited a very small, but real, signal extending sever-

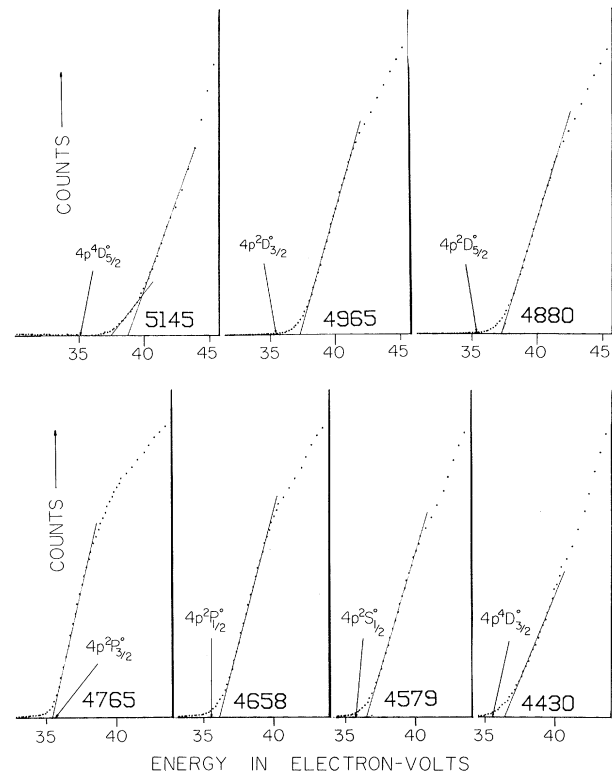


FIG. 1. Relative excitation-function data near threshold. The arrows represent threshold for the single-step noncascade process.

al volts below threshold for process (1). The most plausible explanation of this signal in our experiment consists of a two-step reaction involving charge exchange between neutrals and Ar⁺ ions accelerated in the grid-cathode region. Long, photographic time exposures demonstrated that a small fraction of the total light was emitted in this region, and the magnitude for the charge-exchange cross sections needed to explain the observations through this reaction is quite reasonable in view of the recent work by Lipeles, Novick, and Tolk⁹ on similar processes. (Excitation functions of neutral helium and neon transitions used to calibrate the apparatus indicated that the tail of the electron energy distribution extended only ≈ 0.2 eV above the applied potential.)

The cross-section data shown in Fig. 2 were taken one point at a time using normalization against a standard lamp (calibrated at the National Bureau of Standards) in such a manner that each point represented an absolute measurement. These data were taken at lower and lower currents until the results were indepen-

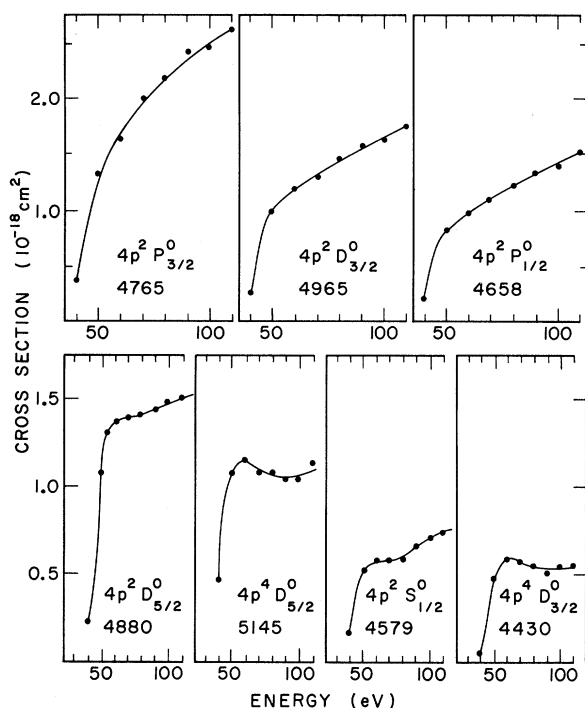


FIG. 2. Absolute single-step excitation cross sections as a function of electron energy. (The wavelengths used to study each state are given in angstroms.)

dent of the current. Data were also taken at several pressures to make sure the cross-section data showed no significant pressure dependence. The data were obtained using pulsed excitation to avoid any detectable effects of ion density. A gated scaler was used with a liquid-nitrogen-cooled photomultiplier tube. In order to avoid any possible calibration errors that might arise from nonlinearities, the signal from the standard lamp was adjusted geometrically to give about the same counting rate as the individual Ar II transitions being measured when observed through the same gated photon-counting system. The solid angle subtended by the standard lamp closely approximated that subtended by the excitation region in the gun. Close agreement was obtained, however, even when the lamp-to-spectrometer distance was changed by a factor of 30. The spectrometer entrance aperture was both small and distant from the electron gun. Precise knowledge of either the aperture size or scaler duty cycle was unnecessary in the calibration procedure. A photographic determination of the excitation-region geometry was made using emission from the Ar II lines. The instrumental linewidth ($\approx 2 \text{ \AA}$) was determined

using the same Ar II transitions, and the spectral region around each line was carefully scanned to make sure that there was no significant contribution from nearby lines. The final limit of error on each cross section is $\approx 20\%$ and represents the rms value of all the independent errors in the experiment. No polarization effects were observable.

The cross section for each state is proportional to R_2/A_{21} , where R_2 represents the total relaxation rate of the upper level of the transition and A_{21} is the individual Einstein A coefficient for the transition. Our previous lifetime data¹⁰ demonstrate that R_2 is closely given by the total radiative decay rate for the pressures used here. The total radiative values were determined experimentally¹⁰ within ≈ 2 to 6% . The ratios in Table I were determined by normalizing new relative intensity measurements for the $4p \rightarrow 4s$ transitions and calculated values¹¹ for the weaker $4p \rightarrow 3d$ lines to the measured¹⁰ total values. This procedure yielded values of the individual A coefficients within $\approx 10\%$ and avoided reliance on the more approximate calculated values for the $4p \rightarrow 4s$ transitions.¹²

Table II gives a comparison of our measured cross sections with values calculated by Koozekanani using the "sudden" approximation. The data are presented as percentage ratios of the excitation cross section to the total ionization cross section at two energies near the maximum (90 eV) in the total ionization cross section. No correction has been made for cascade. Also, in evaluating the ratio $Q_{\text{exc}}/Q_{\text{ion}}$, the uncertainties in the total ionization cross section⁸ are comparable with the uncertainties in our measured values of the individual excitation cross sections. The calculated values in Table II are typically two to three times smaller than the measured cross sections. The dis-

Table I. Inverse branching ratios used to determine the Ar II excitation cross sections.

Transition (λ in \AA)	A_2/A_{21}
4430	2.04
4579	1.73
4658	1.37
4765	1.85
4880	1.29
4965	2.91
5145	18.2

Table II. Comparison of measured values of (Q_{exc}/Q_{ion}) with those calculated by Koozekanani from the "sudden" approximation.

State (λ in Å)	Q_{exc}/Q_{ion} (in percent)		
	Calculated by Koozekanani ^a	Measured ^b	
		90 eV	110 eV
$^2S_{1/2}^{\circ}(4579)$	0.070	0.21	0.23
$^2P_{1/2}^{\circ}(4658)$	0.27	0.41	0.48
$^2P_{3/2}^{\circ}(4765)$	0.26	0.75	0.82
$^2D_{3/2}^{\circ}(4965)$	0.13	0.49	0.55
$^4D_{3/2}^{\circ}(4430)$	0.0014	0.16	0.17

^aRef. 3.

^bPresent work and Ref. 8.

crepancy in all cases is in the direction to be anticipated from cascade. An accurate experimental determination of the cascade contributions would require spectral data from ≈ 0.15 to 1.2μ . However, we note that the 5145-Å line is likely to have its major contribution from cascade, from considerations both of angular orthogonality and of the observed excitation function. Therefore, the observed $^4D_{5/2}^{\circ}$ cross section is a rough measure of the cascade contribution which might be anticipated for any state in (3P) $3p^44p$ configuration. Allowance for a cascade contribution of that general magnitude would give reasonable agreement between the experimental and calculated values in Table II. Some of the discrepancy may, of course, also arise from a failure of the "sudden" approximation in this energy range.

A final object of the present work is to provide some quantitative data related to the fractional involvement of single- and multi-step excitation processes in the conditions actually encountered in a cw argon ion laser. In principle, by comparison of the observed excited-state density, electron density, and measured cross sections one may determine the actual fraction of excited states formed through reaction (1) (including cascade). A comparison of this type has been made in Table III for the strongest three laser transitions. The discharge data correspond to a filling pressure of 0.2 Torr in a 2-mm capillary at 7 A discharge current. The total electron densities and neutral-atom densities were determined from Stark and Doppler width measurements which we reported previously¹³ and from the assumption of Boyle's law. The absolute excited-state

Table III. Percentage of excited-state density observed in a dc argon ion laser which would be due to single-step excitation for an assumed mean electron energy \bar{E} .

\bar{E} (eV)	State (λ in Å)		
	$4p^2P_{3/2}^{\circ}(4765)$	$4p^2D_{5/2}^{\circ}(4880)$	$4p^4D_{5/2}^{\circ}(5145)$
4.0	0.12	0.02	0.02
5.0	2.3	0.6	0.2
6.0	11	4.5	1.4
7.6	100	35	17
8.7	250	100	49
10.1	530	240	100

ion densities¹⁴ were determined from light emitted out the side of the discharge tube in the transitions studied above. The present comparison assumes a Maxwellian electron velocity distribution and has been made for several different mean electron energies. The fact that the mean energies required for 100% yield of upper states observed in the discharge are all different implies that direct excitation cannot be the only process involved. Our data also show that direct electron excitation is most important for the 4765 transition of the three lines in Table III. This conclusion is compatible with consistent differences observed with varying E/p in pulsed-discharge conditions for the relative gain of the 4765 and 4880 transitions⁴ and with the different exponential dependence on current observed by us for these three transitions. For the cw discharge conditions used to obtain the data in Table III, the $^2P_{3/2}^{\circ}$, $^2D_{5/2}^{\circ}$, and $^4D_{5/2}^{\circ}$ excited state densities varied as the 1.8, 2.0, and 2.2 power of the current, respectively, as is compatible with a decreasing fractional importance of the single-step process in going from the $^2P_{3/2}^{\circ}$ to the $^4D_{5/2}^{\circ}$. A final point worth making is that the present data imply that ultimate efficiencies $\approx 0.05\%$ would be obtainable from the direct excitation process in this laser on the 4765-Å transition.

The authors are indebted to Dr. S. Koozekanani for the disclosure of his calculations prior to publication.

*Research supported in part by the U. S. Air Force Office of Scientific Research and the U. S. Army Research Office at Durham.

†To be submitted by G. N. Mercer in partial fulfill-

ment of the requirements for the degree of Doctor of Philosophy at Yale University.

‡Alfred P. Sloan Foundation Fellow.

¹W. R. Bennett, Jr., *Ann. Phys. (N. Y.)* **13**, 367 (1962); discussion on p. 417.

²W. R. Bennett, Jr., J. W. Knutson, Jr., G. N. Mercer, and J. L. Detch, *Appl. Phys. Letters* **4**, 180 (1964).

³S. Koozekanani, *J. Quant. Electron.* **2**, 14 (1966); and to be published.

⁴See W. R. Bennett, Jr., *Appl. Opt. Suppl.* **2**, 3 (1965).

⁵W. E. Lamb, Jr. and M. Skinner, *Phys. Rev.* **78**, 539 (1950).

⁶R. M. St. John and C. C. Lin, *J. Chem. Phys.* **41**, 195 (1964).

⁷See E. I. Gordon, E. F. Labuda, R. C. Miller, and C. E. Webb in *Physics of Quantum Electronics*, edited by P. L. Kelley, B. Lax, and P. E. Tannenwald

(McGraw-Hill Book Company, Inc., New York, 1965), pp. 664-673.

⁸L. J. Kieffer and G. H. Dunn, *Rev. Mod. Phys.* **38**, 1 (1966), Fig. 8.

⁹M. Lipeles, R. Novick, and N. Tolk, *Phys. Rev. Letters* **15**, 815 (1965).

¹⁰W. R. Bennett, Jr., P. J. Kindlmann, G. N. Mercer, and J. Sunderland, *Appl. Phys. Letters* **5**, 158 (1964).

¹¹F. A. Horrigan, S. H. Koozekanani, and R. A. Paananen, *Appl. Phys. Letters* **6**, 41 (1965).

¹²H. Statz, F. A. Horrigan, S. H. Koozekanani, C. L. Tang, and G. F. Koster, *J. Appl. Phys.* **36**, 2278 (1965).

¹³E. A. Ballik, W. R. Bennett, Jr., and G. N. Mercer, *Appl. Phys. Letters* **8**, 214 (1966).

¹⁴These densities were $(1.0, 1.6, \text{ and } 3.6) \times 10^9$ per cm^3 for the ${}^2P_{3/2}$, ${}^2D_{5/2}$, and ${}^4D_{5/2}$, respectively.

LINE PROFILE IN THE ONE-ELECTRON APPROXIMATION*

J. Cooper

Joint Institute for Laboratory Astrophysics,† Boulder, Colorado

(Received 23 September 1966)

The shape $I(\omega)$ of a pressure-broadened line in the classical path approximation is¹

$$I(\omega) = \frac{1}{\pi} \text{Re Tr} \int_0^\infty e^{-i\omega s} \{Z(0)Z(s)\rho_A\}_{\text{av}} ds, \quad (1)$$

where $Z(s)$ and ρ_A are the dipole moment and density-matrix operators, the trace being over states of the perturbed system and the average over perturber coordinates.

In a recent paper by Griem¹ this expression [Eq. (1)] is used to evaluate the electron-impact broadening of isolated ion lines. Griem evaluates the above expression under the assumption that during the time s there is at most the interaction of a single perturber. (This approximation should be well satisfied in the line wings.) In particular, it is implied¹ that this approach takes into account collision-induced transitions between upper and lower levels of the line which are not included in the more usual impact approximation of Anderson² and Baranger.³

It is the purpose of this present note to indicate that this "one-electron approximation"⁴ should give results identical with the impact approximation. This means that some terms

given by Griem¹ [e.g., in his Eq. (8)] should not be included. It is felt that these terms appear because the levels are erroneously chosen as being completely degenerate during the interaction. The "proof" of the equivalence of one-electron and impact approximations is presented in the following.

When using Griem's notation,^{1,5}

$$\begin{aligned} & \{Z(0)Z(s)\rho_A\} \\ &= \{Ze^{-iHs/\hbar}U(s,0)ZU^\dagger(s,0)e^{iHs/\hbar}\rho_A\}, \quad (2) \end{aligned}$$

where H is the Hamiltonian of the Hamiltonian of the unperturbed system. $U(s,0)$ obeys the Schrödinger equation

$$\begin{aligned} i\hbar \frac{dU}{ds}(s,0) &= e^{iHs/\hbar}V(s)e^{-iHs/\hbar}U(s,0), \\ &= V'(s)U(s,0), \quad (3) \end{aligned}$$

where $V'(s)$ is the interaction Hamiltonian.

If there is no interaction between times 0 and s' , then $V'(s) = 0$ and $U(s',0) = 1$. Suppose then a collision occurs between s' and $s' + \Delta s'$; an iterative solution of Eq. (3) gives

$$\begin{aligned} U(s' + \Delta s', 0) &= [1 - (i/\hbar) \int_{s'}^{s' + \Delta s'} ds_1 V'(s_1) + (i/\hbar)^2 \int_{s'}^{s' + \Delta s'} \int_{s'}^{s' + \Delta s'} ds_1 ds_2 V'(s_1) V'(s_2) + \dots] e^{-iHs'/\hbar} \\ &= e^{iHs'/\hbar} [1 - (i/\hbar) \int_0^{\Delta s'} dt_1 V'(t_1) + (i/\hbar)^2 \int_0^{\Delta s'} \int_0^{\Delta s'} dt_1 dt_2 V'(t_1) V'(t_2) + \dots] e^{-iHs'/\hbar}, \quad (4) \end{aligned}$$